Deep Learning based Automatic Fracture Identification in CT Images of Rock

Chuyen Pham
Korea Institute of Civil Engineering and Building Technology, Gyeonggi-do, South Korea
University of Science and Technology, Daejeon, South Korea

Li Zhuang
Korea Institute of Civil Engineering and Building Technology, Gyeonggi-do, South Korea
University of Science and Technology, Daejeon, South Korea

Sun Yeom
Korea Institute of Civil Engineering and Building Technology, Gyeonggi-do, South Korea

Hyu-Soung Shin
Korea Institute of Civil Engineering and Building Technology, Gyeonggi-do, South Korea
University of Science and Technology, Daejeon, South Korea

ABSTRACT: Computed tomography (CT) scans have been widely used to study the internal structure of rock including fractures. However, accurately quantifying fractures based on CT data could be challenging due to blurry appearance of fractures in CT images, complexity of fracture patterns and heterogeneity of the host rock. In this study, deep learning-based method is presented for automatically and accurately segmenting fractures in CT images of rock. The method involves two steps: fracture detection using the Faster R-CNN algorithm and fracture segmentation using the U-Net algorithm. The detection step establishes spatial constraints for the segmentation process, significantly removing noise and artifacts in background and improving the final segmentation result. CT images of fractured granite, sandstone and shale were applied for verifying the proposed method. It was found that our method can achieve a Dice score of up to 0.93, outperforming other deep learning approaches including Mask R-CNN or U-Net alone.

Keywords: Rock fracture, Computed tomography, Deep learning, Rotated bounding box.

1 INTRODUCTION

Many studies have shown that the mechanical and hydraulic properties of fractures determine the stability and permeability of a rock mass. Thus, the accurate characterization of fracture is critical for safe and cost-effective implementation of different rock engineering projects including natural resource exploration and production, hazardous waste disposal, tunneling and underground construction. Recent advancements in computed tomography technology make it the most effective method for analyzing the internal structure of human body and industrial materials such as concrete, steel as well as rock (Andrä et al., 2013). Beyond visualization, CT scan also allows for extraction of the geometry of a region of interest through segmentation process. Despite the fact that the segmentation process has received extensive research, segmentation of narrow planar features such as fractures in CT images remains a challenging task, owing to the limitation of CT image resolution, the presence of artifacts and the blurriness of fracture in the images due to the partial volume effect (Iassonov et al., 2009; Johns et al., 1993). So far, several approaches have been proposed to overcome these problems (Deng et al., 2016; Voorn et al., 2013), but these all suffer from the restrictions of

Hessian-based filter relating to variation in fracture scale, the low-contrast of fracture and the heterogeneity of background (Lee et al., 2021). Since these methods frequently fail to provide satisfactory result, manual post-processing is typically required. This is not only time-consuming but also costly because a set of CT data may compose of thousands of CT images. Recently, the success of deep learning models was highlighted in many fields for their capability to perform complex computer vision tasks including image classification and segmentation at the level of specialist. This study proposed an ensemble deep learning approach, which integrates our recent study using rotated Faster R-CNN deep learning model for fracture detection with a variant of U-Net deep learning model to provide a fully-automatic pipeline for fracture segmentation in CT images with high accuracy.

2 METHODOLOGY

Our approach consists of two steps: (1) Fracture detection in form of minimal bounding boxes, and (2) Fracture segmentation in each detected bounding box (Figure 1). In the first step, a modification of Faster R-CNN deep learning algorithm is implemented to detect the fracture in an image with rotated bounding boxes. The outputs of this network are the location, size and orientation of bounding boxes encompassing the fractures. Sequentially, an encoder-decoder deep learning convolutional neural network so-called U-Net is adopted to produce a pixel-wise segmentation of fracture within each detected bounding box. The benefits of this approach will be examined in depth in the discussion section.

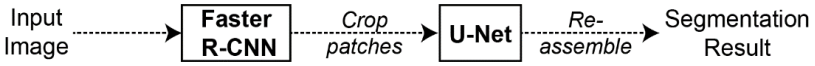

Figure 1. Complete pipeline for fracture segmentation.

2.1 Faster R-CNN

Faster R-CNN is a region-based object detection deep learning algorithm, which is built up of three primary components: the backbone network, the region proposal network, and the region-based convolution neural network (R-CNN) (Ren et al., 2015). The backbone network is a combination of ResNet-101 and FPN to extract multi-level feature maps from an input image (Lin et al., 2017). The RPN then uses these feature maps and predefined anchor boxes to propose up to 512 bounding boxes that likely enclose fractures. Finally, those proposed bounding boxes are used to crop and resize the feature maps before passing them through the final component R-CNN. The R-CNN has several convolution layers with two fully connected layer branches as outputs for classification and further box coordinates refinement via bounding box regression. The detail of Faster R-CNN architecture and operation is discussed in our recent work (Pham et al., 2021). The major difference in our implementation from the original Faster R-CNN is the use of rotated bounding boxes. When compared to the typically used bounding box (i.e., axis-align bounding box), the rotated bounding box is more adaptable to the elongated and directional fractures, thus reducing the background ratio within the bounding box more effectively.

2.2 U-Net

U-Net is a deep learning algorithm developed for medical image segmentation, which architecture composes two symmetrical paths: a contraction path and an expansion path (Ronneberger et al., 2015). The contraction path uses convolutional blocks to gradually downscale the input image to learn the context in the input image. The expansion path, on the other hand, employs deconvolutional blocks to gradually upscale the feature maps back to the original size of the input image and classify each pixel into two classes (i.e., fracture and non-fracture pixel). The introduction of skip connections in U-Net is the major innovation that made it possible to segment fine-scale features. The skip connection acts as a bridge between the contraction and expansion paths, allowing to pass feature

maps from the contraction path to the expansion path. This aids in the recovery of spatial information that has been lost owing to pooling procedures during the downscaling process. In this study, we employ a variant of U-Net known as Residual Attention U-Net to segment fracture in the detected bounding box. This variant adds an attention gate to each level of skip connection (Oktay et al., 2018) and substitutes the usual convolutional block with a residual block (i.e., ResNet-34's component). These two modifications allow the network to learn more complex patterns and to focus the segmentation process on specific parts of the image where relevant features exist rather than the full image, resulting in a significant boost in segmentation accuracy.

2.3 Data and experiment

2.3.1 Dataset

CT image datasets used in this study were acquired from the scanning of artificially fractured granite, sandstone and shale cylinders. The CT images are visualized in grayscale with intensity values ranging from 0 (black – low-density material) to 255 (white – high-density material). As seen in Figure 2a, the fractures appear as dark and torturous lines with varied thicknesses throughout their length. A total of 800 CT images was manually annotated fracture with rotated bounding boxes to train the Faster R-CNN (Figure 1a). Only 450 out of the 800 images were pixel-wise labeled for the fracture to train the U-Net (Figure 1b). All images were pre-processed with Non-local Means Filter and Contrast Limited Adaptive Histogram Equalization before further analysis to eliminate noise and also enhance phase contrast.

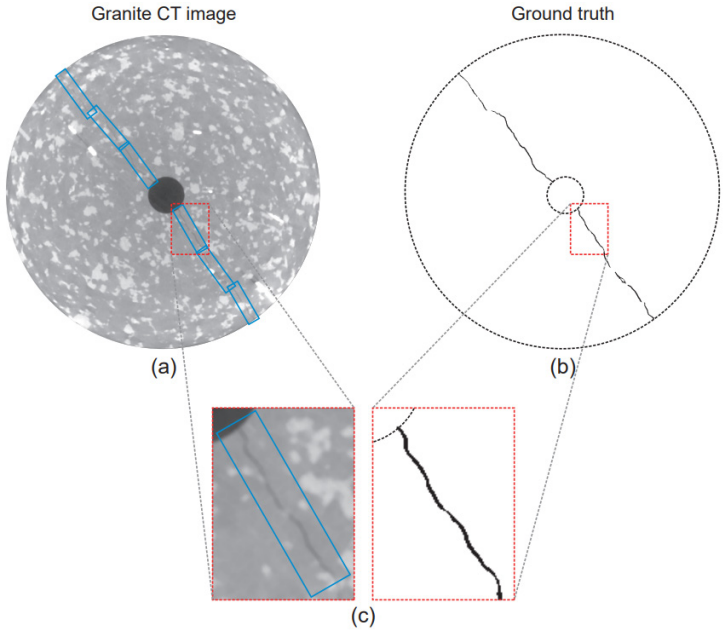

Figure 2. An example of input image: (a) CT image with rotated ground truth bounding boxes (blue), (b) Corresponding ground truth segmentation of the CT image, (c) zoom-in images within red boxes.

2.3.2 Experiment

We implement the networks in Python using an open-source platform for machine learning TensorFlow and train them separately. For the Faster R-CNN network, we leave aside 100 images for testing whereas the rest is used for training (600 images) and validation (100 images). All images are resized to 640×640 before feeding to the network. The stochastic gradient descent algorithm with an initial learning rate of 0.0001 was used for optimizing the model across 100 epochs, which took around one and a half-day after the loss remained steady. The loss function is described in Ren et al. (2015). About hyperparameters, the longest side scales of the anchor box are set to (16, 24, 32, 40,

48) pixels with aspect ratios of (2, 1/2, 3, 1/3, 5, 1/5) and the orientations evenly distributed from 0° to 90° in 15° increments, while the other hyperparameters are kept the same as (Ren et al., 2015). In the context of U-Net, 450 images were split into three portions of 280 images, 70 images, and 100 images for training, validation, and testing, respectively. These CT images were cropped into patches based on the ground truth bounding boxes and then padded with zero padding to a fixed size of 256×256 as a requirement of the same size input image of U-Net. The network is trained for 100 epochs using Adam optimizer with an initial learning rate of 0.0001. A weighted sum of Dice and binary cross-entropy losses is utilized as the loss function. In the test phase, Faster RCNN and U-Net are assembled to seamlessly obtain the final segmentation result.

3 RESULT AND DISCUSSION

The fracture detection and segmentation results on the test set are used to evaluate the performance of our approach. Examples of qualitative results are shown in Figure 3. The detection step is assessed using the mean average precision (mAP) metric with a threshold of 0.5, whereas the segmentation step is evaluated using the Dice score metric. Both metrics range from 0 to 1, with a higher value indicating higher agreement between prediction and ground truth. As shown in Table 1, the Faster R-CNN model has a high mAP of 0.897, indicating that the model can effectively detect fractures in unseen images. In combination with Faster R-CNN, the U-Net model obtain an average Dice score of up to 0.932 on the test set. We also implemented each of Mask R-CNN and U-Net on the same dataset for comparison purposes. The comparative results show that our proposed approach outperforms the standard U-Net and Mask R-CNN for the test set. It clearly notices that Dice score gains of 7.9% and 26.1% when compared to U-Net and Mask R-CNN, respectively. This improvement can be attributed to two following factors. First, rather than considering the whole image, the segmentation process is limited to the interior of the detected bounding box, which significantly alleviates the complexity of the background. Second, cropping patches according to rotated bounding box for training not only mitigates the class imbalance between fracture and background, but also augments the size of the datasets that significantly improve the model generalization. Despite the certain increase in computing time, our suggested approach outperformed other conventional deep learning algorithms (i.e., Mask R-CNN, U-Net) with the same cost of segmentation ground truth annotation, making it a superior alternative to cope with the problem of a small dataset.

Table 1. Performance of fracture segmentation using the different approaches.

Model	mAP@0.5	Dice score	Inference time (sec/image)
U-Net	-	0.864	0.97
Mask R-CNN	0.886	0.739	1.38
Faster R-CNN + U-Net	0.897	0.932	2.42

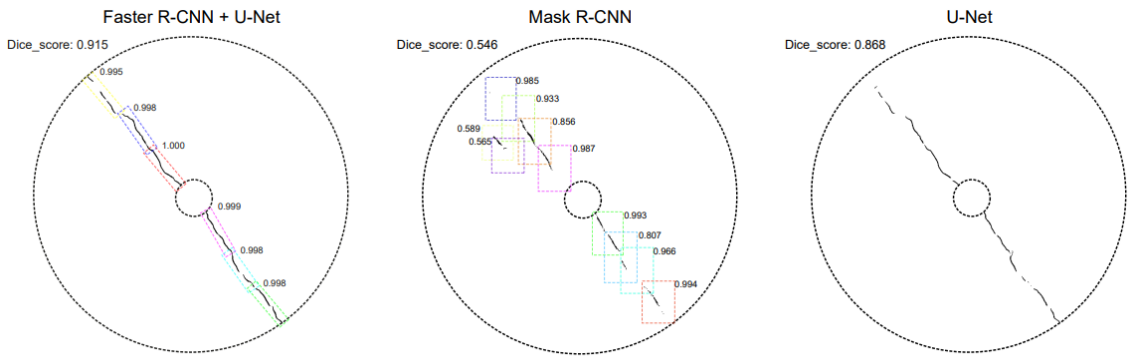

(a)

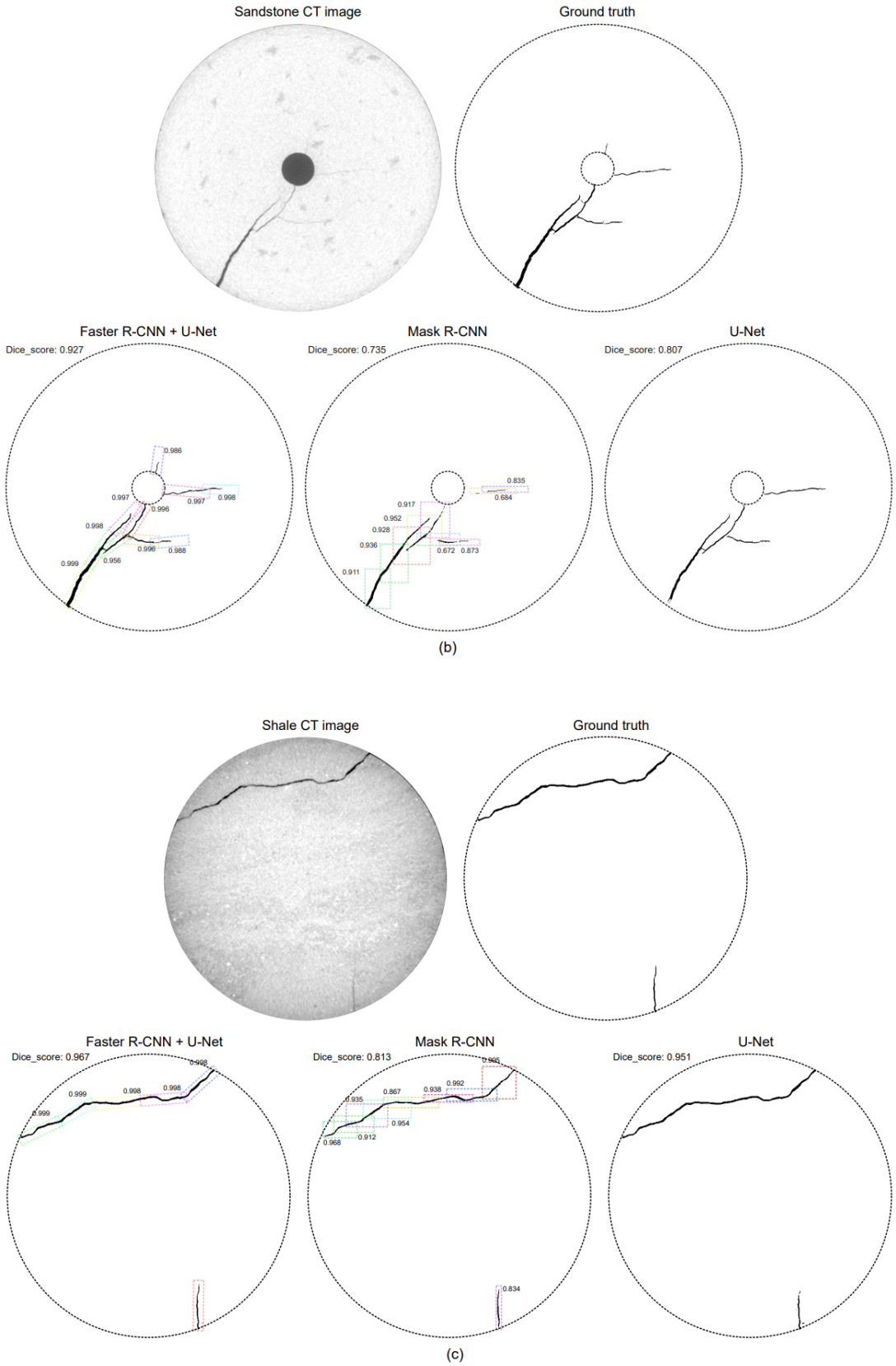

Figure 3. Examples of the segmentation results of the proposed approach and others. (a) Segmentation result of granite CT image shown in Figure 2a, (b, c) Segmentation result of sandstone and shale CT images, respectively.

4 CONCLUSION

Our proposed approach achieves remarkable success in dealing with segmenting fractures in rock CT images. To address the inherent difficulties in fracture segmentation on CT images, our method first localizes fractures in CT images with the rotated bounding box and then segments fracture in each detected bounding box in the second step. The prior spatial constraints obtained from the fracture detection step significantly contribute to the improvement in segmentation performance. Although our approach has limitations in training and inference time, it outperforms other deep learning algorithms and is also considerably faster than manual attempts. To some extent, this method is also applicable for detecting cracks or fractures in buildings, roads, tunnels, and other structures.

ACKNOWLEDGMENTS

This research was supported by the project "Development of environmental simulator and advanced construction technologies over TRL6 in extreme conditions" funded by KICT.

REFERENCES

Andrä, H., Combaret, N., Dvorkin, J., Glat, E., Han, J., Kabel, M., Keehm, Y., Krzikalla, F., Lee, M. & Madonna, C. 2013. Digital rock physics benchmarks–Part I: Imaging and segmentation. Comput. Geosci. 50:25–32.

Deng, H., Fitts, J.P. & Peters, C.A. 2016. Quantifying fracture geometry with X-ray tomography: Technique of iterative local thresholding (TILT) for 3D image segmentation. Computational Geosciences. 20(1):231–244.

He, K., Gkioxari, G., Dollár, P. & Girshick, R.B. 2017. Mask R-CNN. CoRR.

Iassonov, P., Gebrenegus, T. & Tuller, M. 2009. Segmentation of X-ray computed tomography images of porous materials: a crucial step for characterization and quantitative analysis of pore structures. Water Resour Res. 45(9):1–12.

Johns, R.A., Steude, J.S., Castanier, L.M. & Roberts, P.V. 1993. Nondestructive measurements of fracture aperture in crystalline rock cores using X-ray computed tomography. Journal of Geophysical Research. 98:1889–1900, doi: 10.1029/92JB02298.

Lee, D.W., Karadimitriou, N., Ruf, M. & Steeb, H. 2021. Detecting micro fractures with X-ray computed tomography. [Preprint]. arXiv:2103.12821.

Lin, T., Dollár, P., Girshick, R.B., He, K., Hariharan, B. & Belongie, S.J. 2017. Feature pyramid networks for object detection. CVPR.

Oktay, O., Schlemper, J., Le Folgoc, L., Lee, M., Heinrich, M., Misawa, K., et al. 2018. Attention U-Net: learning where to look for the pancreas. [Preprint]. arXiv: 1804.03999.

Pham, C., Zhuang, L., Yeom, S. & Shin, H.S. 2021. Automatic Fracture Detection in CT Scan Images of Rocks Using Modified Faster R-CNN Deep-Learning Algorithm with Rotated Bounding Box. Tunnel and Underground Space, 31(5), 374-384.

Ren, S., He, K., Girshick, R. & Sun, J. 2015. Faster R-CNN: Towards real-time object detection with region proposal networks. In: NIPS.

Ronneberger, O., Fischer, P. & Brox, T. 2015. U-Net: Convolutional Networks for Biomedical Image Segmentation. MICCAI, Springer, LNCS. 9351:234-241.

Voorn, M., Exner, U. & Rath, A. 2013. Multiscale Hessian fracture filtering for the enhancement and segmentation of narrow fractures in 3D image data. Comput Geosci. 57:44–53. doi:10.1016/j.cageo.2013.03.006.